24th INTERNATIONAL CONGRESS ON SOUND AND VIBRATION
23–27 July 2017, London

ICSV24
23-27JULY 2017
LONDON CALLING

ON EVOLUTION OF INTENSE ACOUSTIC NOISE. THEORY AND EXPERIMENT

Sergey Gurbatov*, Mikhail Deryabin, and Vasiliy Kurin

Nizhny Novgorod State University, Nizhny Novgorod, Russia
e-mail: gurb@rf.unn.ru

Dmitry Kasyanov

Institute of Applied Physics, Nizhny Novgorod, Russia

Propagation of noise acoustic beams at high Reynolds numbers is investigated theoretically and experimentally. From a mathematical point of view the problem of describing the spread of noise is reduced to finding the statistical characteristics of solutions of Burgers equation. Narrow-band input noise field can be regarded as quasi-monochromatic signal with random amplitude and phase modulation. Away from radiator the field represents the sequence of shocks with the universal behaviour between shocks. The positions of the shocks and their amplitude and, hence, the statistical characteristics of the waves are determined by the fluctuations of the phase of the initial wave. It is shown that at large distances the field spectrum has the universal structure defined by the initial wave statistics. The nonlinear interaction leads to the initiation of new harmonics, the width of which increases with the number of harmonics, and a continuous power spectrum is formed at high frequencies. The evolution of noise intensive acoustic beams at high Reynolds numbers with narrowband spectrum inlet is experimentally studied (signal with central frequency 2 MHz and with an initial amplitude P about 1 MPa). Experiments were carried out using measuring complex Ultrasound Measurement System Control Centre by Precision Acoustics. The details are investigated of the spatial and temporal structure of the acoustic beams at high Reynolds numbers and the spectral content of the field is analyzed up to the fortieth harmonic of radiation source. It is shown experimentally the appearance of universal high-frequency asymptotic behaviour.
Keywords: (nonlinearity, noise, acoustic beam, Burgers)

1. Introduction

Interest to studying the propagation of intense acoustic noise is sufficiently keen, for example, the studies of noise created by the modern-aircraft engines in the audio-frequency range are very topical [1-4]. Description of propagation of intense noise is usually based on solving the Burgers equation, which was proposed by J.M.Burgers as a model equation of hydrodynamic turbulence. Random fields satisfying this equation are called the Burgers turbulence and even Burgulence [5] or acoustic turbulence as applied to evolution of intense acoustic noise. Many works (e.g., see the references in the monographs and reviews [5-13]) are dedicated to the studies of the statistical characteristics of intense acoustic noise and Burgers turbulence. The laboratory experiments include the studies of harmonic oscillation by the noise quasi-monochromatic signal at the initial stage [14] and intense-noise propagation in pipes [15-17].

The studies presented in this work deal with propagation of intense ultrasonic noise beams in fluid for large Reynolds numbers. The results of analytical calculation of the spectra of the noise

narrowband signals at the stage of the developed discontinuities are given along with the results of the experimental study of evolution of noise acoustic beams.

2. Evolution of the plane quasi-monochromatic waves

Currently, the most exhaustive description of propagation of an intense acoustic field in the paraxial approximation can be obtained within the framework of the Khokhlov--Zabolotskaya--Kuznetsov (KZK) equation [6, 18]. However, the solution of this equation, especially for complex initial and boundary conditions, is sought numerically and usually lacks proper physical demonstrativeness. Therefore, to ensure a high-quality consideration of the peculiarities of evolution of the quasi-periodic signals, we consider the one-dimensional Burgers equation:

$$\frac{\partial v}{\partial z} - v\frac{\partial v}{\partial t} = \Gamma \frac{\partial^2 v}{\partial t^2}. \tag{1}$$

When writing (1), the following dimensionless variables are used:

$$v = \frac{p}{p_0}, z = \frac{x}{l_{SH}}, t = \omega_* \tau \ . \tag{2}$$

Here, p is the acoustic pressure, x is the coordinate along the beam axis, and τ is the time in the coordinate system moving together with the wave with the sound velocity c_0. Variables (2) are normalized to the amplitude value of the pressure p_0, the characteristic wave frequency ω_0, and the nonlinear length l_{SH}, which is the distance at which a discontinuity in the plane wave that is harmonic at the input is formed. The characteristic distances at which the discontinuities and dissipative effects are formulated as

$$l_{SH} = \frac{c_0^3 \rho_0}{\varepsilon\, \omega_0\, p_0}, \ l_{DISS} = \frac{2 c_0^3 \rho_0}{b\, \omega_0^{\ 2}}. \tag{3}$$

The ratio of these lengths forms the dimensionless number $\Gamma = l_{SH} / l_{DISS}$, which is the inverse acoustic Reynolds number (Goldberg number). Note that Eq. (4) can also be used for describing propagation of the spherical waves in the case of the vanishingly small viscosity ($\Gamma \to 0$).

Narrowband noise can be represented as a quasi-monochromatic signal:

$$v_0(t) = a(t)\cos(\omega_* t + \varphi(t)), \tag{4}$$

where $a(t)$ and $\varphi(t)$ are the functions describing the random amplitude and phase modulations. In the dimensionless variables (2), the amplitude and the frequency ω_* are of the order of unity. Let us consider the statistical characteristics of the wave in the case $z >> 1$, such that initially it is assumed that $\Gamma \to 0$ and the shock fronts have an infinitesimal width. Therefore, it is obvious that the quasi-monochromatic wave is transformed into a sequence of the sawtooth triangular pulses with the same slope $v_z^{'} = -1/z$ and the initial amplitude modulation is suppressed in the medium. Profile of the sawtooth wave, and, consequently, the statistical characteristics are entirely determined by the coordinates of "zeros" and shocks.

The sawtooth-wave "zeros" coincide with the initial-signal zeros and are obtained from the equation:

$$\omega_* t_n + \varphi(t_n) = \pi/2 + 2\pi n, n = 0, \pm 1, \pm 2, ... \tag{5}$$

For the narrowband signal, the discontinuity amplitude $\Delta U_n(x)$ and its coordinate $\tau_n(x)$ are expressed in terms of the derivatives of the amplitude, phase, and frequency [19,20]. In this case,

we confine ourselves to the quasistatic approximation when the discontinuity motion can be neglected. In this approximation, we neglect the energy pumping down the spectrum. In this case, for the amplitude of the discontinuity $\Delta U_n(x)$ and its coordinate $\tau_n(x)$ we have:

$$\Delta U_n = (t_{n+1} - t_n)/z, \quad \tau_n \approx (t_{n+1} + t_n)/2. \tag{6}$$

Equations (5) and (6) show that the sawtooth wave has both the amplitude modulation, which is related to the discontinuity-amplitude fluctuations, and the phase modulation due to the discontinuity-location fluctuations. The discontinuity-amplitude fluctuations are due to the input-signal frequency fluctuations $\Omega(t) = \partial\varphi(t)/\partial t$

$$\Delta U_n \approx (t_{n+1} - t_n)/z \approx \Delta U_*(z)[1 - \frac{\Omega(t_n)}{\omega_*}], \quad \Delta U_*(z) = \frac{2\pi}{z\omega_*}. \tag{7}$$

To analyze the energy spectrum of the field $v(t,z)$, it is convenient to consider the derivative $\partial v(t,z)/\partial t$, which is a sequence of the delta-shaped pulses with the amplitude and coordinates equal to those of the discontinuity. Assuming the initial process to be stationary and using the well-known relationships for the spectrum of the sequence of the pulsed signals for the spectral density $S(\omega,x)$ of the field $v(t,x)$, we write the following relationship [17,20]:

$$S(\omega,x) = \frac{1}{\omega^2}\left[\frac{\omega_*}{4\pi^2}\sum_{p=-\infty}^{p=\infty}\left\langle \Delta U_{k+p}\Delta U_k \exp[-i\omega(\tau_{k+p} - \tau_k)]\right\rangle - \frac{1}{z^2}\delta(\omega)\right], \tag{8}$$

where δ is the Dirac delta function.

Since for the quasi-monochromatic signals, the discontinuity-amplitude fluctuations are relatively small and can be neglected in the first approximation, for $S(\omega,x)$ we have:

$$S(\omega,x) = \frac{\Delta U_*^2}{4\pi^2}\frac{\omega_*}{\omega^2}\left[1 + \sum_{\substack{p=-\infty \\ p\neq 0}}^{p=\infty}\left\langle \exp[-i\omega(\tau_{k+p} - \tau_k)]\right\rangle\right]. \tag{9}$$

Here, the averaging is performed over the random discontinuity locations τ_k. This formula determines the energy spectrum of the field as a sum of the interference terms among the Fourier transforms of individual discontinuities. Interference at various frequencies leads to either a decrease or increase in the spectral density $S(\omega,x)$ compared with the spectral density of an individual discontinuity, which is proportional to $\Delta_*^2 U(z)/\omega^2$. For a harmonic input signal, discontinuity locations are determinate and the spectral density is discrete:

$$S(\omega,x) = \sum_{\substack{k=-\infty \\ k\neq 0}}^{k=\infty} A_k^2 \delta(\omega - k\omega_*), \quad A_k^2 = \frac{\Delta U_*^2}{4\pi^2}\frac{1}{k^2}. \tag{10}$$

For the quasi-monochromatic signal, the bandwidth $\Delta\omega_k$ at each field harmonic increases with the harmonic number and the bands of individual harmonics merge for $\Delta\omega_k >> \omega_*$. In this case, the interference of the spectra of individual harmonics can be neglected and only the first term remains in (9). Comparing expressions (9) and (10), we see that the noise-spectrum fall-off law $S(\omega,x) \propto \omega^{-2}$ coincides with the law $A_k^2 \propto k^{-2}$ of fall-off of the squares of the amplitudes of harmonics with their numbers increasing. In this case, the ratio of the spectral density of noise in the frequency band $\Delta\hat{\omega}$ to the squared amplitude of the k harmonic equals $S(k\omega_*)\Delta\hat{\omega}/A_k^2 = \Delta\hat{\omega}/\omega_*$ and is frequency-independent [17].

Since the phase fluctuations for the quasi-monochromatic signal are small in the period, we write $\tau_{n+p}-\tau_n \approx t_{n+p}-t_n$ and to determine the spectral density (see expressions (8) and (9)), it is sufficient to know the coordinates of the sawtooth-wave zeros. Equation (5) for the coordinates t_n of the sawtooth-wave zeros has no exact solution and various approximations should be used during the statistical analysis [20]. Here, we consider the case of large and slow frequency departures when the main contribution to the sum in Eq. (9) is from the first terms and to determine the distances between the fronts, one can be confined to the first term in the expansion $\varphi(t_{k+p})-\varphi(t_k) \approx \Omega(t_k)(t_{k+p}-t_k)$ of the phase difference. As a result, we obtain:

$$\sum_{\substack{p=-\infty \\ p\neq 0}}^{p=\infty} \left\langle \exp[-i\omega(\tau_{k+p}-\tau_k)] \right\rangle \approx \sum_{\substack{p=-\infty \\ p\neq 0}}^{p=\infty} \left\langle \exp[i\omega \frac{2\pi p}{\omega_*}\frac{\Omega}{\omega_*} - i\omega\frac{2\pi p}{\omega_*}] \right\rangle. \tag{11}$$

The mean in (11) is determined by the characteristic function $\theta_\Omega(\lambda)=\langle \exp(i\lambda\Omega)\rangle$ of the frequency Ω. Using the Poisson summation formula [21], one can easily pass from summation over the interference terms of the Fourier transforms of individual discontinuities (see expressions (8), (9), and (11)) to summation over the harmonic numbers. As a result we obtain that the spectral-line form is determined by the form of the probability distribution $W_\Omega(\Omega)$ of the frequency and repeats its form for the narrowband signals. In particular, for the Gaussian probability distribution with dispersion $\overline{\Omega^2}$, we write the following expression:

$$S(\omega,x)=\frac{\Delta U_*^2}{4\pi^2}\frac{\omega_*^2}{\omega^2}\left[\sum_{\substack{n=-\infty \\ n\neq 0}}^{n=\infty} \frac{1}{\sqrt{2\pi\overline{\Omega^2}}}\frac{\omega_*}{\omega}\exp\left(-\frac{(\omega-n\omega_*)^2}{2\overline{\Omega^2}}\frac{\omega_*^2}{\omega^2}\right)\right]. \tag{12}$$

For sufficiently narrowband signals in the sum (12), one can replace $\omega_*/\omega \approx 1/n$, where n is the harmonic number. The harmonic bandwidth $\Delta\omega_n \approx n\sqrt{\overline{\Omega^2}}$ increases with the harmonic number and for $\Delta\omega_n >> \omega_*$ the individual-harmonic lines merge. In this case, a continuous spectrum which is proportional to ω^{-2} and determined by the first term in formula (9) is formed. Allowance for the amplitude fluctuations leads to weak asymmetry of the harmonic spectrum, which is due to the fact that the amplitude and frequency fluctuations are anticorrelated, i.e., the amplitude decreases with increasing frequency.

For finite, but sufficiently large Reynolds numbers, the form of the shock fronts coincides with that of the stationary shock front and their dimensionless width σ is $\sigma = 2\Gamma\omega_*^2 z/\pi$ [7]. This leads to appearance of the multiplier $K(\omega,z)=(\omega\pi\Gamma/2\omega_*)^2/sh^2(\omega\pi\Gamma/2\omega_*)$ in the expressions (8), (9), and (12) for the spectral density, which describes the exponential "cutting" of the spectrum, i.e., $K \approx \exp(-\omega\pi\sigma/\omega_*)$ for $\omega >> \omega_*/\sigma$.

The analytical estimates given above are obtained in the one-dimensional approximation. Nevertheless, as is shown below, they sufficiently accurately describe evolution of the intense noise paraxial beams featuring the nonmonotonous dependence of the field amplitude in the beam axis on the distance and asymmetry of the positive and negative peak values of the discontinuity amplitude [13,18,23,24], which is related to the diffraction effects. The results of the experimental studies given below show that the diffraction effects at the developed-discontinuity stage lead to insignificant difference of the field-spectrum behavior from the power law $S(\omega,x) \propto \omega^{-2}$. Moreover, one can observe a sufficiently good agreement of the experimentally measured spectra with the theoretical results given in expression (12).

3. Experimental study of evolution of the noise beams

The experimental facility (the flow-diagram is given in Fig. 1A) is based on the measurement complex produced by company Precision Acoustics (Ultrasound Measurement System Control Centre) and includes an organic-glass container *1* with the dimensions 1x1x1m, manipulators for hydrophone and radiator, control computer, and oscillograph Agilent DSO-X 3034 *2*. The absolute accuracy of motion along the three coordinates ***x, y, z*** using the manipulators is 6 mcm. The container was filled by a very clean degassed and deionized water with a specific resistance of at least 18 MOhm*cm, which was produced by the DM-4B membrane distiller unit (Russia). The water temperature was controlled by a thermometer and amounted to 22±0.1°C in the experiments. The profile of intense acoustic waves was recorded by the membrane PVDF hydrophone (DH0902) *3* manufactured by company Precision Acoustics. This hydrophone has a characteristic size of the sensing element of 0.2 mm (the sensing element is manufactured of the 9 mcm thick PVDF film) and is calibrated in the frequency range up to 40 MHz by the manufacturer . The nonuniformity of the sensitivity characteristic in this frequency range does not exceed 20%.

The radiating part of the facility consists of Tektronix AFG3022 driving two-channel oscillator *4*, Amplifier Research 800A100A power amplifier *5*, IT2001 Amplifier Research impedance adapter *6*, and radiator *7*. The plane piezoceramic radiator manufactured by Olympus company was used in the experiments. The radiator operation frequency and the aperture radius were 2 MHz and 2 cm, respectively. The radiator Q-factor did not exceed three. Using the oscillator, the noise signal in the wide frequency range was created, while the already narrowband noise, which was determined by the amplitude-frequency characteristic of the radiator, was radiated to the medium. The pump signal was monitored by the oscillograph via the measuring probe (Voltage probe Tektronix P6139B).

The signal received from the hydrophone was supplied to the Power Supply preamplifier *8* produced by Precision Acoustics company, preanalyzed by the Agilent DSO-X 3034 oscillograph, and recorded to the computer.

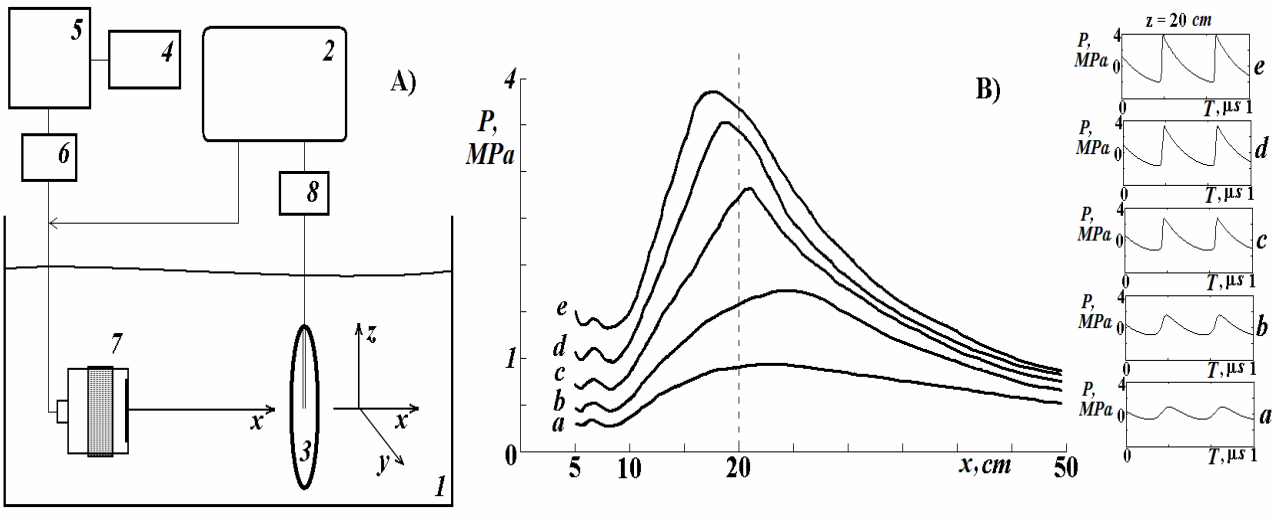

Figure 1: A) Experimental facility flow diagram; B) Amplitudes of the acoustic-wave compression front along the acoustic axis *x* for five various input amplitudes at the radiator aperture P_0 : a – 0.3 MPa, b – 0.4 MPa, c – 0.6 MPa, d – 0.8 MPa, and e – 1MPa).

The measurements were conducted on the radiator acoustic axis x. During the measurements, the hydrophone was motionless, while the radiator moved along the acoustic axis. The automated complex allows one to perform detailed measurements of the acoustic-field structure. In the experiments, the field was measured in a distance range of 50 - 500 mm from the initial aperture.

The features of the paraxial propagation of an intense acoustic beam is demonstrated in Fig. 1B. The main attention should be paid to the nonmonotonous behavior of the compression front of an acoustic wave along the acoustic axis ***x***. Figure 1B shows the corresponding distributions for five various initial pressure amplitudes. These dependences are obtained in the radio-pulse radiation mode with a basic frequency of 2 MHz.

The dependences shown in Fig. 1B obviously demonstrate the saturation effect of the shock-front amplitude at large propagation distances. A successive increase in the pressure amplitude at the initial radiator aperture does not lead to a proportional increase in the shock-front amplitude at a large distance from the radiator aperture. However, in the described experimental environment, full saturation is not reached because of the limited nature of the Reynolds numbers and propagation distance.

Let us note another manifestation of the joint action of diffraction and nonlinearity. Once the initial-aperture pressure is increased, the maximum of the compression front of the wave is first displaced from the radiator and then starts to move to the latter (see Fig. 1B). The coordinate of the maximum of the compression front in an intense acoustic beam is determined by both the Reynolds acoustic number and the radiator diffractive properties. For demonstrativeness, the wave profiles recorded at the distance ***x*** = 20 cm from the radiator aperture are shown in the right-hand part of Fig. 1B for various pressure amplitudes at the initial aperture. This distance corresponds to the last diffraction maximum in the field distribution, which is created by the used radiator during its operation in the linear mode. During insignificant manifestation of nonlinear effects (case "a"), the coordinate of the compression-front maximum is in the region of the last diffraction maximum. In case "b," the nonlinear effects already lead to formation of the shock front and the shock-front formation coordinate is located behind the last diffraction maximum. Approaching the distance ***x*** = 20 cm, the shock front is formed only in cases "c", "d," and "e", such that the compression-front maximum moves closer to the initial aperture with increasing P_0 and the "saturation effect" is also observed.

The experiment on studying the intense-noise evolution along the acoustic axis was organized as follows. The digital oscillator created the time realization of white noise. This realization was recorded and supplied to the radiator via the amplification circuits individually for each spatial location of the radiator--hydrophone system.

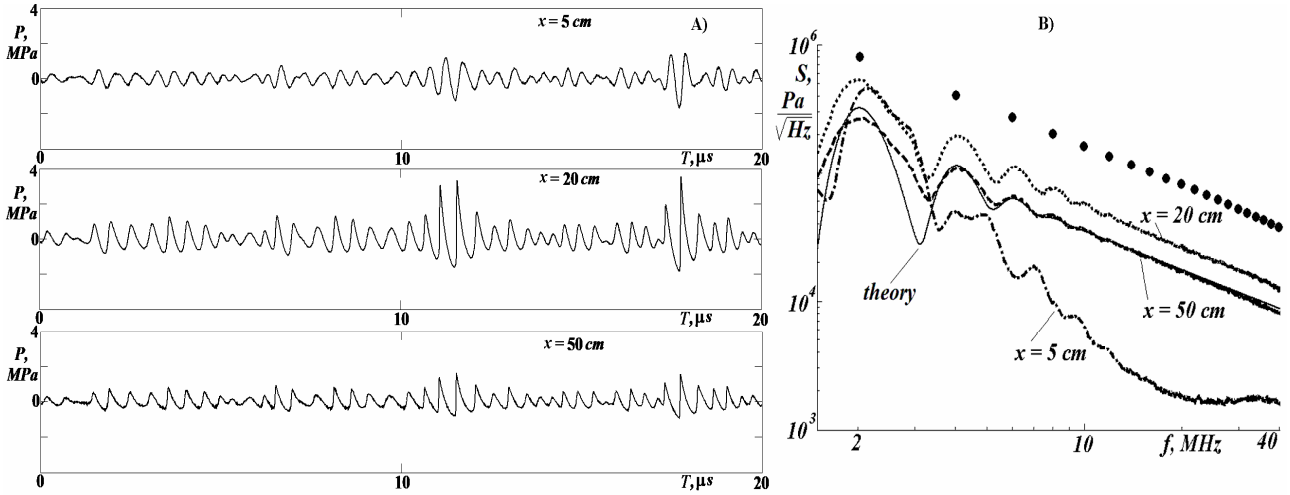

Figure 2: A) Oscillograms of the noise signals at the distances from the radiator equal to x = 5 cm, x = 20 cm, and x = 50 cm; B) The noise-signal spectra and the amplitudes of the tone-signal harmonics at the distances ***x*** = 5 cm, ***x*** = 20 cm, and ***x*** = 50 cm from the radiator in the log-log scale. The solid line is used to denote the theoretical dependence obtained using expression (12).

Figure 2A shows the characteristic oscillograms. At short distances from the radiator aperture, the shock fronts in the noise-beam profiles have no time to be formed. Approaching the distance ***x*** =

20 cm, the shock fronts are formed in the profiles of the most high-amplitude parts of the beam realizations. Approaching the propagation distance $\boldsymbol{x}$ = 50 cm, the shock fronts are formed in the majority of the sections of the noise-beam profile such that the trend to the amplitude-modulation suppression is observed as it was theoretically predicted. In this experimental environment, no complete equalization of the overoscillation amplitudes is observed because it is necessary to reach large Reynolds numbers in the beam or long distances, which is beyond the potential of the used experimental equipment.

To study the spectral characteristics of the noise signal at each considered spatial coordinate, 1000 oscillograms with durations of 20 mcm were recorded. The spectra were taken from each oscillogram. Then the averaged spectrum of the noise signal was calculated at the considered spatial point over all realizations.

Figure 2B shows the spectra of the recorded noise signal, while the amplitudes of the tone signal harmonics (2MHz, P_0=1MPa) at the distances $\boldsymbol{x}$ = 5 cm, $\boldsymbol{x}$ = 20 cm, and $\boldsymbol{x}$ = 50 cm from the radiator are given for comparison. The dependences in Fig. 2B are given in the log-log scale with the frequency and the spectrum amplitude laid off as abscissa and ordinate, respectively. The solid line in Fig. 2B is used to denote the theoretical dependence obtained from expression (12) by parametric adjustment.

Therefore, the experiment has shown that despite the diffractive features of evolution of intense acoustic beams, the plane-wave theory sufficiently well describes the form of the noise-signal spectrum at the discontinuous stage. In this case, the spectrum of the noise quasi-monochromatic signal can be described by the above-given analytical expressions.

4. Acknowledgments

This work was supported by grant No. 14-12-00882 of the Russian Scientific Foundation.

REFERENCES

1 Morfey, C.L. and Howell, G.P., *Nonlinear propagation of aircraft noise in the atmosphere*, AIAA J. 19, 986–992 (1981).

2 Gee, K.L., Gabrielson, T.B., Atchley, AA., and Sparrow, V.W., *Preliminary analysis of nonlinearity in military jet aircraft noise propagation,* AIAA J. 43, 1398–1401 (2005).

3 Crocker, M.J. Ed., *Handbook of Noise and Vibration Control*, John Wiley & Sons, Hoboken, NJ (2007).

4 Gee, K.L., Sparrow, V.W., James, M.M., Downing, J.M, Hobbs, C.M., Gabrielson, T.B., and Atchley, A.A., *The role of nonlinear effects in the propagation of noise from high-power jet aircraft*, J. Acoust. Soc. Am. **123** (6), 4082-4093, (2008).

5 Frisch, U., Bec, J., *Burgulence. New trends in Turbulence*, Les Houches 2000, pp.341- 383. Springer EDP-Sciences, (2001).

6 Rudenko, O.V., Soluyan, S.I. *Nonlinear acoustics.* New York, Pergamon Press, (1977).

7 Gurbatov, S.N., Saichev, A.I. and Yakushkin, I.G., Nonlinear waves and one-dimensional turbulence in nondispersive media, *Sov. Phys. Usp.* **26(2)**, 221-256, (1983).

8 Gurbatov, S.N., Malakhov, A.N. and Saichev, A.I. *Nonlinear Random Waves and Turbulence in Nondispersive Media: Waves, Rays, Particles,.* Manchester University Press, (1991).

9 Rudenko, O.V., Interactions of intense noise waves, *Sov Phys Usp.*, **29** (7), 620–641, (1986).

10 Rudenko, O.V., Nonlinear sawtooth-shaped waves, *Phys-Uspekhi*, **38** (9), 965–989, (1995).

11 Gurbatov, S.N., Rudenko, O.V., *Statistical Phenomena*, Ch. 13 in the Book: Nonlinear Acoustics (Ed. by M.F.Hamilton and D.T.Blackstock) Academic Press, New York, (1998)

12 Bec, J., Khanin, K., Burgers turbulence, *Physics Reports*. **447**, (2007).

13 Gurbatov, S.N., Rudenko, O.V., Saichev, A.I., *Waves and Structures in Nonlinear Nondispersive Media. General Theory and Applications to Nonlinear Acoustics,* Springer-Verlag and HEP, (2011).

14 Pernet, D.F., Payne, R.C., Nonlinear propagation of signals in air, *J. Sound and Vib.* **17**, 383–387 (1971).

15 Pestorius, F.M. and Blackstock, D. T., Experimental and theoretical study of propagation of finite-amplitude noise in a pipe, in *Finite-Amplitude Wave Effects in Fluids*, edited by L. Bjorno **,** IPC Science and Technology Press, Ltd., Guildford, UK, (1973**)**.

16 Sakagami, K., Aoki, S., Chou, I.M., Kamakura, T., Ikegaya, K., Statistical characteristics of finite amplitude acoustic noise propagating in a tube, J. Acoust. Soc. Jpn. (E) 3, 43–45 (1982).

17 Bjorno, L., Gurbatov, S.N., On establishment of high-frequency asymptotic under propagation of intense acoustic noise, *Sov. Phys. Acoust.* **31**, (1985)

18 Rudenko, O.V., The 40th Anniversary of the Khokhlov-Zabolotskaya Equation, *Acoust.Phys*. **56**. (4), 457-466, (2010).

19 Gurbatov, S.N., Malakhov A.N., On statistical characteristics of random quasi-monochromatic waves in nonlinear media, *Sov. Phys. Acoust*. 23, 325–331 (1977).

20 Gurbatov, S.N. and Shepelevich, L.G., *Spectra of discontinuous noise waves*, *Radiophys Quantum Electron*, 21(11), 1131–1138, (1978),

21 Feller, W., *Introduction to Probability Theory and Its Applications*, Vol. 2, Wiley (1971).

22 Gurbatov, S.N., Deriabin, M. S., Kasyanov, D.A. and Kurin, V.V., Degenerate parametric interaction in powered acoustic beams , *Radiophys Quantum Electron*, **59**(10), (2016).

23 Andreev, V. G.; Karabutov, A. A.; Rudenko, O. V., Experimental study of the propagation of nonlinear sound beams in free space, *Soviet Physics - Acoustics*, **31** (4), 252-255, (1985).

24 Sapozhnikov O., Khokhlova V., Cathinol D., Nonlinear waveform distortion and shock formation in the near field of a continuous piston source, *J. Acoust. Soc. Am.*, **115** (5), 1982 – 1987, (2004).